An original pure bending device with large displacements and rotations for static and fatigue tests of composites structures

Tarak Ben Zineb, Ara Sedrakain, Jean-Louis Billoët

An original pure bending device with large displacements and rotations for static and fatigue tests of composite structures

Tarak Ben Zineb[a,*], Ara Sedrakian[b], Jean Louis Billoet[b]

[a]*LPMM, U.M.R CNRS 7554 ISGMP ENSAM Metz, 4, rue Augustin Fresnel 57078 Metz, cedex 3, France*
[b]*LMSP, U.M.R CNRS 8106 ENSAM Paris, 151 Boulevard de l'Hôpital, 75013 Paris, France*

As composite structures, flexible structures have, for pure bending loading, significant displacements and rotations. The design and the dimensioning of these structures require good material characterization beyond the small deformations domain. This paper thus proposes a new original device making pure bending loading possible in large transformations. The sample is embedded at each end using a sleeve with a rigid body movement. The applied bending moment is perfectly controlled during the loading. A behavior model of the bench based on the beam theory for large transformations is developed, making it possible to dimension and design this bench. An experimental campaign using glass/epoxy composite samples has validated this new device in static and fatigue states. This device was used for identification of a fatigue model dedicated to flexible composite structures.

Keywords: Mechanical testing; Numerical analysis; Layered structures; Fatigue

1. Introduction

The increasing use of non-conventional materials such as composites or memory-shape alloys for the design and manufacture of structures subjected to large transformations, in particular bending, requires controlling their mechanical behavior throughout loading. Identification of the behavior parameters and their evolution under the effect of non-linear mechanisms such as hyperelasticity, plasticity or damage becomes not easy to control with traditional experimental devices. They very quickly generate disturbance phenomena. It will not be possible to control the piloting parameters during the test and to identify behavior thresholds.

These identification problems are increased in the case of analyzing heterogeneous materials such as the composites whose mechanical characteristics are strongly anisotropic. This anisotropy can generate, in the case of disturbance loading, the evolution of damage.

* Corresponding author. Tel.: +33-3-87-37-54-34; fax: +33-3-87-37-54-70.
E-mail address: tarak.benzineb@metz.ensam.fr (T. Ben Zineb).

This paper highlights problems encountered during the characterization of beam or plate parts subjected to bending loading, in particular, beyond small deformations. Bending is one of the major modes of loading for many structures. It is the subject of many identification mechanical tests such as three-point bending, four-point bending, etc. These tests, however, generate complex strain and stress states. Identification of material constants becomes difficult. In the case of composite material parts, whose shearing properties are very low compared to those in the normal direction, a premature cracking due to the side effects of the test modify interpretation of the results.

Our research relates to the design and the validation of a pure bending bench in large displacements and large rotations greater than 30°, more particularly intended for identification of composite material characteristics in static and fatigue states.

The control of pure bending loading has many advantages:

- The uniformity of the stresses in reference planes gives a large flexibility of instrumentation, in particular for the strain state assessment.

- The control of the strain skew-symmetry if tension and compression behaviors are the same. If not, this makes it possible to study the differences and to predict better the thresholds of damage and the associated mechanisms.
- In small deformations, small displacements and rotations, the system most used for pure bending loading is the four-point bending bench. It is very difficult to generalize the use of this bench, in its state, to the case of large displacements and rotations. Indeed, this generalization induces difficulties related to the control and the piloting of applied bending moment as well as the boundary conditions.

Taking this device as a starting point and cross the difficulties it induces in finite transformations, we studied, designed and developed an original device. It making it possible to load samples or structures in pure bending, while having significant displacements and rotations, without losing control of the boundary conditions and the monitoring parameters.

The unit, defined by the pure bending device in finite transformations, is composed of two parts. The first one is undeformable and has a perfectly controlled rigid body movement with the possibility of displacement monitoring. The second one is deformable and corresponds to the useful part of the structure loaded in pure bending. To study the behavior of the deformable part, we used the large transformation beam theory developed by SIMO [3–5]. Concerning the rigid part, we used the traditional kinematic relations corresponding to rigid body movement. We supplemented this study by a finite element analysis leading to the exact dimensioning of this rigid part.

2. Critical analysis of conventional 4-point bending devices

2.1. Presentation

The conventional four-point bending bench makes it possible to obtain, in the case of small loading, pure bending stresses (BC area, Fig. 1). The sample is simply posed on two supports and a system of swing bars imposes two concentrated forces with equal intensity symmetrical compared to the sample median plane. By a simple mechanical calculation, we can prove that the BC area, Fig. 1, is loaded in pure bending. The two other areas have a nonzero shear stress. The bending moment applied in the BC area is constant and entirely defined by the applied load intensity and distance between the support and the load application point.

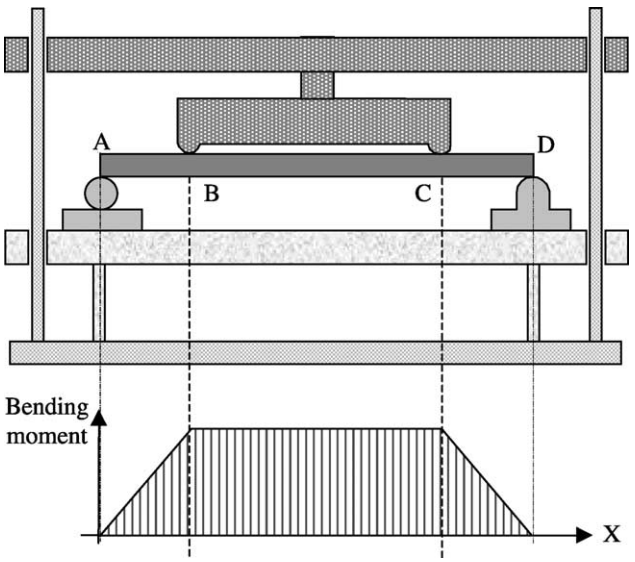

Fig. 1. Traditional bending device.

2.2. Critical analysis

The four-point bending benches are very well adapted for materials and structures whose high rigidity allows behavior analysis for small deformations.

Behavior analysis of flexible structures under a pure bending loading by using this type of conventional benches induces quite a few disadvantages. They affect the quality of the achieved results and, in certain cases, distorts them completely. The principal disadvantages of these assemblies [1,8] are

- The supports, as well as the load application points, are fixed. They cannot thus follow the deformed structure profile. This generates a normal force on the structure and a slipping of the support. Consequently, the central part is not loaded in pure bending.
- For materials having low shear strength, a premature rupture can appear at the level of the AB and CD areas, Fig. 1. This is more probable since the ratio AB over the sample length is weak.
- To calculate the bending moment at any loading step, the distance between the support and the application load point must be known as well as the direction of the force. Indeed, these two parameters, if they remain constant for small deformations, evolve during large displacements and rotations.
- Near the supports, the contact is linear. It induces locally a high stress concentration leading to a premature failure in the case of brittle structures such as any composite part.
- At the supports, the sample rotates around an axis displaced compared to the horizontal median plane. In the case of small deformations, this does not have an influence on the quality of the test. In large displacements and rotations, this shift becomes disturbing.

In order to resolve these various defects and problems for the analysis of flexible parts, we designed an original pure bending bench. The following paragraph describes the design steps and the characteristics of this new bench.

3. Pure bending bench in large transformations

3.1. Principle

The schedule of design conditions of this new bench clarifies the following points:

- The zone of measurement requested in pure bending must be the most significant possible.
- The applied bending moment must be controlled throughout external loading, even in the large geometrically non-linear phase.
- The applied load must absolutely avoid secondary stresses, like transverse shearing or disturbing normal forces usually due to fixed supports.
- The risks of premature rupture due to stress concentrations at the level of support lines or the loading areas must be avoided.
- The support rotation must be significant and carried out around the median plane of the sample.

3.2. Technological description of the new device

A rigid part on the both sides of the sample, Fig. 2, directly resolves several points of condition schedule. The bending moment is transmitted by a contact surface between the sample and the rigid part. The jack and supports forces are directly applied to this rigid part. A rotation around an axis, which belongs to the sample medium plane, is obtained. Moreover, the supports as well as the points of application forces have a displacement in the longitudinal direction. Applied forces remain vertical during the loading. It may be assumed that friction existing in the contact domain remains very weak. Thus the flexible part is only loaded by a bending moment with the advantage of being quantifiable. This quantification during loading is obtained by knowing the geometry of the rigid part and the control parameters (force and displacements induced by the tensile test machine).

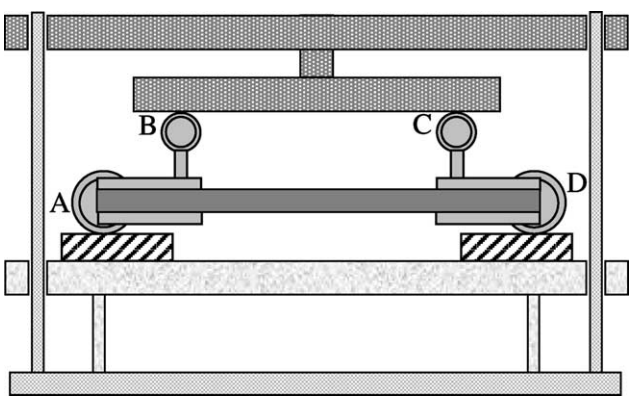

Fig. 2. Kinematic diagram.

3.3. Study of the device behavior

The device/sample system is compared to a beam structure made of two parts. The first is infinitely rigid. Its behavior is identified starting from a kinematic calculation. The second is deformable. Its behavior is defined by a beam theory for large transformations developed by Simo [2–5].

The device is symmetrical compared to the vertical median plane. Moreover, the loading is uniform along the sample width. The study is done in the (x, y) plane, Fig. 3. Thanks to the symmetry, only one half of the device following the length is considered. Finally, the following assumptions for modeling are adopted:

- Small strains associated with a linear elastic behavior.
- Geometrical non-linear approach taking large displacements and rotations into accounts.
- All the device displacement movements are obtained by bearing without sliding.
- The reactions at supports and loading application points remain vertical during loading.

Equilibrium equations of the rigid part are outlined (Eq. (1)). The rigid part is subjected to the action of the swing bar at the point B, the support reaction at point A and the generalized stresses expressing the effect of the deformable part in point O, Fig. 4. All the quantities are algebric, and the forces (generalized stresses) are expressed in the current configuration.

$$\begin{cases} N_0 = 0 \\ T_0 = 0 \\ M_0 = \dfrac{F}{2}(a\cos\psi_0 - D\sin\psi_0) \end{cases} \tag{1}$$

Where N_0, T_0, M_0, are successively the normal force, the shear force and the bending moment of the cross-section border between the rigid part and the flexible one. The rotation of the rigid part is defined by the jack displacement and the device geometry. Indeed we have:

$$\begin{cases} \sin(\alpha + \psi_0) = \dfrac{D + U_{\text{Jack}}}{\sqrt{a^2 + D^2}} \\ \operatorname{tg}\alpha = \dfrac{D}{a} \end{cases} \tag{2}$$

$$\psi_0 = \arcsin\left(\frac{D + U_{\text{Jack}}}{\sqrt{a^2 + D^2}}\right) - \operatorname{arctg}\left(\frac{D}{a}\right) \tag{3}$$

Displacements and the bending moment transmitted to the deformable part corresponding to the useful area can be

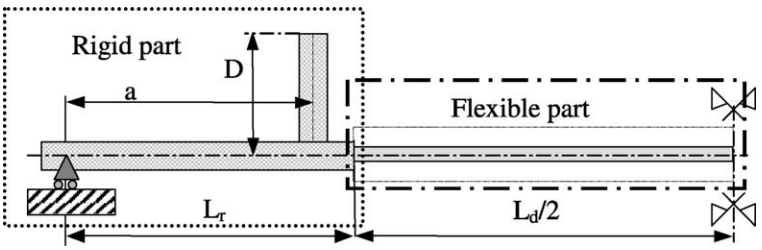

Fig. 3. Whole device and sample.

identified. The equilibrium equations in the static state are used. The sample is compared to a beam. In the gravity center of a given cross-section with the x-co-ordinate x, Fig. 4, the generalized stresses are

$$\{T\}_{\mathrm{G}} = \begin{Bmatrix} N \\ T \\ M \end{Bmatrix} \Rightarrow \begin{cases} 0 \\ 0 \\ \dfrac{F}{2}(a\cos\psi_0 - D\sin\psi_0) \end{cases} \tag{4}$$

The external forces are then identified with the generalized stresses.

Simo in [3–5] presented a beam generalized constitutive law taking into account large transformations with small strains. The equivalent homogeneous behavior is assumed to be isotropic transverse. In a such case the expression of the constitutive law is:

$$\begin{cases} N = \langle E_{\mathrm{L}} S\rangle\left(\left(1+\dfrac{\mathrm{d}u}{\mathrm{d}X}\right)\cos\psi + \dfrac{\mathrm{d}v}{\mathrm{d}X}\sin\psi - 1\right) \\ T = \langle G_{\mathrm{LT}} S\rangle\left(\dfrac{\mathrm{d}v}{\mathrm{d}X}\cos\psi - \left(1+\dfrac{\mathrm{d}u}{\mathrm{d}X}\right)\sin\psi\right) \\ M = \langle E_{\mathrm{L}} I_{zz}\rangle\dfrac{\mathrm{d}\psi}{\mathrm{d}X} \end{cases} \tag{5}$$

With $\langle E_{\mathrm{L}} S\rangle$ and $\langle G_{\mathrm{LT}} S\rangle$ indicating tension and shearing stiffness for the cross-section. $\langle E_{\mathrm{L}} I_{zz}\rangle$ indicates the bending stiffness of the cross-section. The combination of Eqs. (4) and (5) gives

$$\begin{cases} \left(1+\dfrac{\mathrm{d}u}{\mathrm{d}X}\right)\cos\psi + \dfrac{\mathrm{d}v}{\mathrm{d}X}\sin\psi - 1 = 0 \\ \dfrac{\mathrm{d}v}{\mathrm{d}X}\cos\psi - \left(1+\dfrac{\mathrm{d}u}{\mathrm{d}X}\right)\sin\psi = 0 \\ \langle E_{\mathrm{L}} I_{zz}\rangle\dfrac{\mathrm{d}\psi}{\mathrm{d}X} = \dfrac{F}{2}(a\cos\psi_0 - D\sin\psi_0) \end{cases} \tag{6}$$

The boundary conditions of the system are

- Rigid body movement at O.

$$\begin{cases} u(X=0) = u_{\mathrm{A}} - L_{\mathrm{r}}(1-\cos\psi_0) \\ v(X=0) = L_{\mathrm{r}}\sin\psi_0 \\ \psi(X=0) = \psi_0 \end{cases} \tag{7}$$

  where u_{A} is the longitudinal displacement of point A and is to be determined
- Symmetry at $x = L_{\mathrm{d}}/2$.

$$u\left(X=\frac{L_{\mathrm{d}}}{2}\right) = 0 \qquad \text{and} \qquad \psi\left(X=\frac{L_{\mathrm{d}}}{2}\right) = 0 \tag{8}$$

Combination of the relations Eqs. (6)–(8) allows us to describe completely the displacement field of any

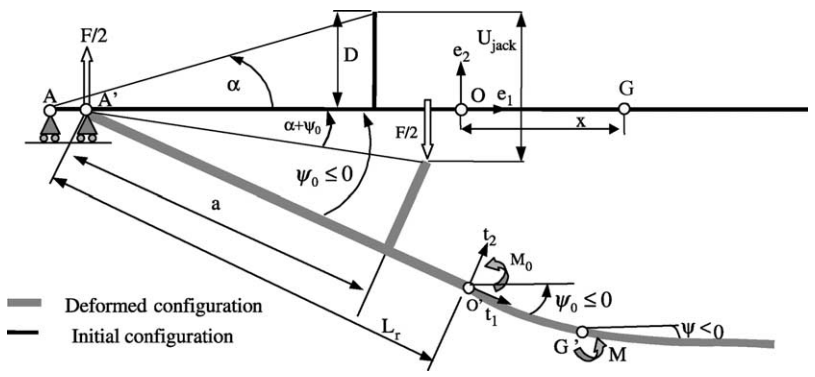

Fig. 4. Rigid part and flexible parts.

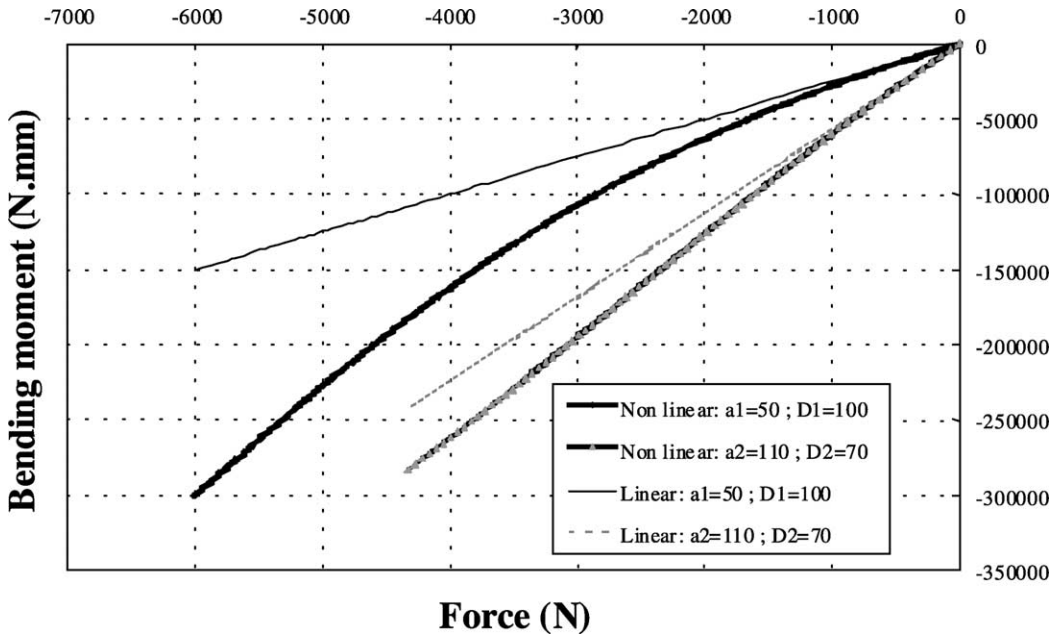

Fig. 5. Influence of geometrical parameters (a, D) in mm.

cross-section. This field is defined by:

$$\begin{cases} u = \dfrac{1}{\omega}(\psi - \sin\psi) \\ v = \dfrac{1}{\omega}(\cos\psi - \cos\psi_0) + L_{\mathrm{r}}\sin\psi_0 \\ u_{\mathrm{A}} = L_{\mathrm{r}}(1 - \cos\psi_0) + \dfrac{1}{\omega}(\psi_0 - \sin\psi_0) \end{cases} \tag{9}$$

$$\text{with } \omega = \frac{2\psi_0}{L_{\mathrm{d}}}, \quad \psi = \psi_0 - \omega X$$

By using the third equation of the system (6), we thus have:

$$\langle E_{\mathrm{L}} I_{zz}\rangle\omega - \frac{F}{2}(a\cos\psi_0 - D\sin\psi_0) = 0 \tag{10}$$

The numerical resolution of Eq. (10) makes it possible to determine of the rotation evolution during loading related to the rigid body movement. The deformation of any cross-section of the flexible part is thus defined by Eqs. (9) and (10). The longitudinal strain for any section of the deformed part is defined by:

$$\epsilon_{xx} = \psi_0\left(\frac{2Y}{L_{\mathrm{d}}}\right) \tag{11}$$

This strain is directly proportional to the rotation of the rigid part and inversely proportional to the length of the deformed part.

The relations Eqs. (1), (3) and (10) show that the bending moment transmitted to the sample depends only on the geometrical parameters of the device (a, D) and on the control parameters of the tensile test machine (F, U_{Jack}). Control of the applied bending moment is obtained by knowing and controlling the geometrical parameters, which remain constant during loading, and the control parameters, as well as force and displacement applied by the jack. A sensitivity study shows the influence of the geometrical parameters. Fig. 5 shows that, according to the values taken by these parameters, the bench behavior can become more or less non-linear and consequently careful attention must be paid, at design step, to defining these quantities. Control parameters (F, U_{Jack}) are defined by the experimenter and the test machine. However, at the design stage, limits are introduced for device dimensioning.

4. Design of a new pure bending device

A condition schedule was established for the device design in Section 3. From this condition schedule we adopted a design stage consisting in bringing a specific solution to each point in order to reach the complete solution.

Other conditions, not mentioned in Section 3, are added in the condition schedule to eliminate the parasitic phenomena induced by the adopted solution. These conditions are

- The measurement of the experimental bending moment. It is defined by the third relation of the system (4). The rotation of the rigid part is calculated starting from jack displacement and the sleeve geometry, Fig. 4. The expression is defined by relation (3).
- The rigid sleeves should not damage the structure especially at the level of the section borders. This constraint was respected thanks to the introduction of two intermediate polymer plates. This solution

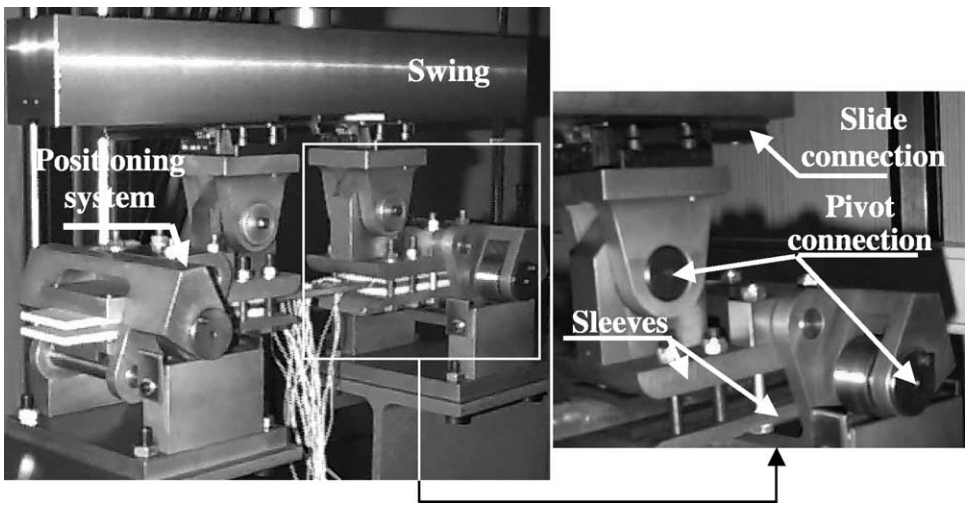

Fig. 6. Pure bending device in finite transformations.

determining the border position between the rigid and the flexible part more difficult. A numerical step, validated experimentally, is presented below. It allowed us to determine the position of the border for a given tightening.

- The device must make it possible to test of samples with different thicknesses while maintaining support rotations around an axis belonging to the sample medium plane. To resolve this problem we introduced an additional part, Fig. 6, making it possible to position the sample and to adapt the sleeve position automatically before starting tightening.
- The sample, when it has a very low thickness, should not be affected by the specific weight of the device. The adopted solution consists in binding the device to the test machine using an additional connection slide between the swing bar and the higher part of two sleeves, in addition to the pivot connections on the supports and the application load points. For brittle samples inducing an abrupt rupture, this solution protects the device from a possible bursting, thus ensuring a protected environment test.
- For dimensioning the various components of the device, we have limited the jack maximum force as well as its maximum displacement.

The summary of this design stage is presented in Fig. 6. It is a system with rigid sleeves posed on supports using linear bearings and connected to the swing bar by two jaws. They ensure the free rotation at the loading points about a connection slide authorizing the free longitudinal displacement of these points. The tightening and the positioning of the upper and lower sleeves are ensured by a positioning part, Fig. 6, and holding-down bolts. Thus it is completely possible to subject the sample to significant displacements and rotations in pure bending loading without losing the control of the pilot parameters, in particular the applied bending moment. The values of the geometrical parameters retained for this design are $a = 112$ mm, $D = 68.5$ mm, $L_r = 115$ mm, $L_d = 150$ mm, Fig. 4.

5. Local analysis of the clamped areas

A global solution masks the existence of a complex stress state in the embedded areas of the sample. This state is due to a discontinuity of rigidity at the transit area between a very rigid part and another rather flexible one. Moreover, uncertainty reigns on the exact position of the border between the rigid part and the flexible one accentuated by the presence of an intermediate polymer part. The goal of this analysis is to identify this position and to make sure that the stress state in the tightening area does not damage the sample.

For this study we developed a finite element model. We adopted the plane stress assumption along to the width. The finite element code used is Abaqus. We used isoparametric solid elements (CPS4 and CPS3) in plane stress and with linear interpolation. They have four or three nodes and two d.o.f (degree of freedom) per node. Calculations are made using a displacement approach, linear elasticity and geometrical non-linearity. The model is composed of four parts:

- The sample is assumed to admit a transverse isotropic behavior.
- An upper and lower sleeves with isotropic behavior. Their stiffness is largely greater than those of the samples.

Table 1
Characteristics of various components

Part	E_L (MPa)	E_T (MPa)	υ_{LT}	G_{LT} (MPa)	G_{TT} (MPa)
Sample	40,000	8,500	0.3	3,340	3,010
Sleeves	210,000	210,000	0.3	80,000	80,000
Plates	5000	5000	0.3	1923	1923
Screws	210,000	210,000	0.3	80,000	80,000

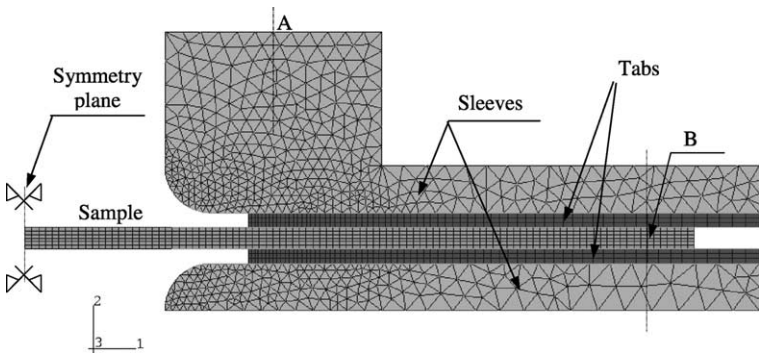

Fig. 7. Meshing and boundary conditions.

- Two isotropic polymer plates.
- Fastening-screws, modeled using beam elements and having an isotropic and very rigid behavior.

Table 1 gives the coefficients for each adopted constitutive law.

With the interfaces between the sleeves and the polymer plates, like on the level of those between the sample and the polymer plates, we introduced contact elements with small slide to take into account the real contact existing in these areas. The boundary conditions imposed are (Fig. 7):

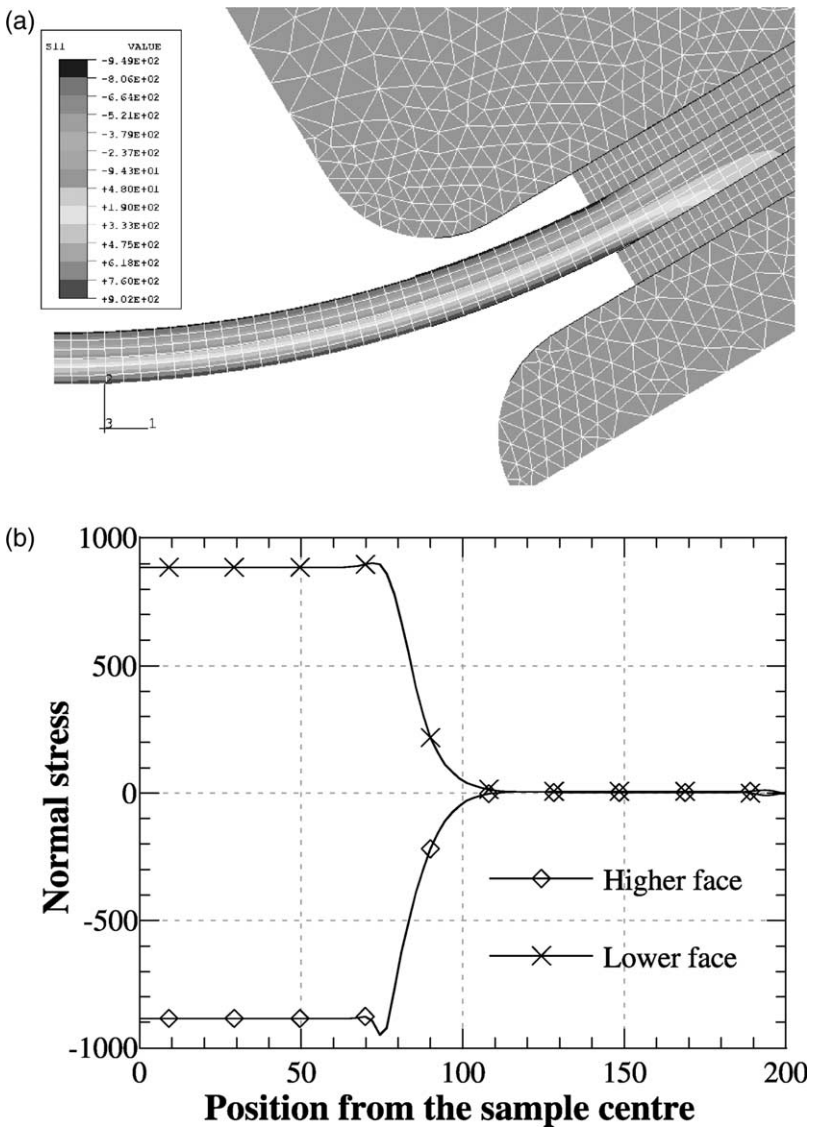

Fig. 8. (a) Normal stress; (b) evolution of the normal stress versus the sample length.

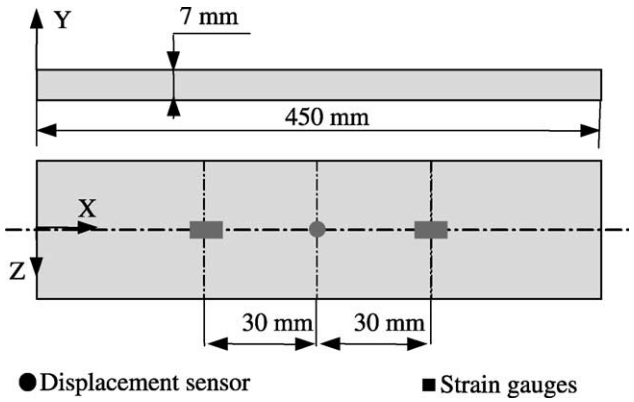

Fig. 9. Sample and instrumentation description.

- an imposed displacement on point A, representing the action of the swing bar;
- a zero longitudinal displacement for the symmetry section.
- Point B is clamped following the transverse direction to represent the support.

The adopted meshing and boundary conditions are described on Fig. 7. Triangular elements are used for the sleeves with a refinement in the zones with high gradient stresses. Quadrangular elements are used for the sample and the polymer plates by adopting the same strategy of refinement.

The longitudinal normal stresses are uniform along the length direction and linear along the thickness, Fig. 8 a and b. Shear and normal transverse stresses are equal to zero in the flexible part. This corresponds to a pure bending stress state. A transition area exists and for which the longitudinal normal stress passes from the nominal value to zero. The longitudinal normal stress is about 950 MPa.

The flexible area extends beyond the limit from tightening. We considered the border, between the flexible part and the rigid one, the section from which a fall of the longitudinal normal stress is noted. This value is used in the calculation of the behavior using the beam theory in finite transformations developed in the above paragraphs. An experimental verification will be carried out for this value.

6. Experimental validation

The device that we presented is especially designed for flexible samples. The length of the sample and the constitutive material must make significant displacements and rotations possible while having rather small strains. Sufficiently long structures in composites with glass fibres check this condition perfectly.

We chose a glass−epoxy composite for the validation of this device. The samples are cut out in a laminated plate manufactured using the Resin Transfer Moulding (RTM) process. The fibres are unidirectional and oriented in the longitudinal direction. The composite is assumed to admit an equivalent homogenized isotropic transverse behavior. The constitutive law coefficients are defined in Table 1. In addition to the measurement of the displacement and jack applied force, we set up an acquisition system making it possible to validate the developed model and especially to check the pure bending stress state of the sample. This system is composed of

- Displacement sensors measuring the maximum deflection and rotation sensors measuring support rotations.
- Strain gauges at various positions of the sample. They are laid out in an optimal way making it possible to measure the strain distribution along the three directions.

Fig. 9 presents the shape of the sample as well as the position of the strain and displacement sensors.

Static tests are carried out with the instrumentation described above. The test machine is a 100 KN hydraulic press. Monitoring is in displacement. For the static tests the velocity is equal to 0.5 mm/s.

From direct observations, we noted during the test (Fig. 10)

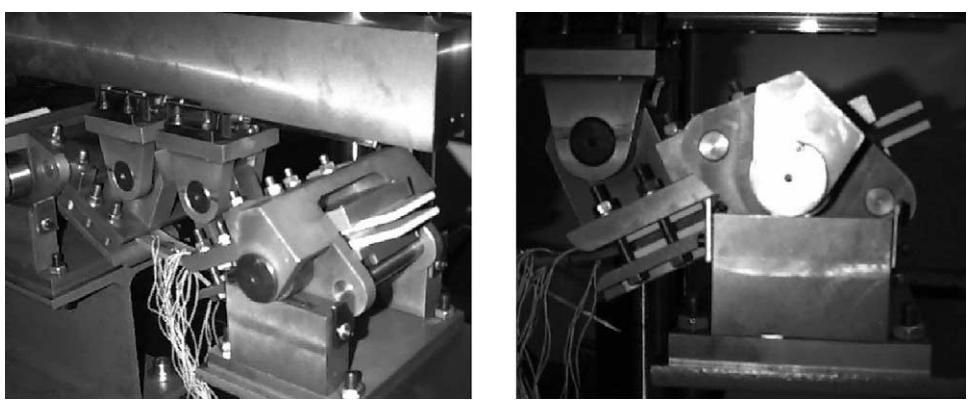

Fig. 10. Deformed sample and support rotations.

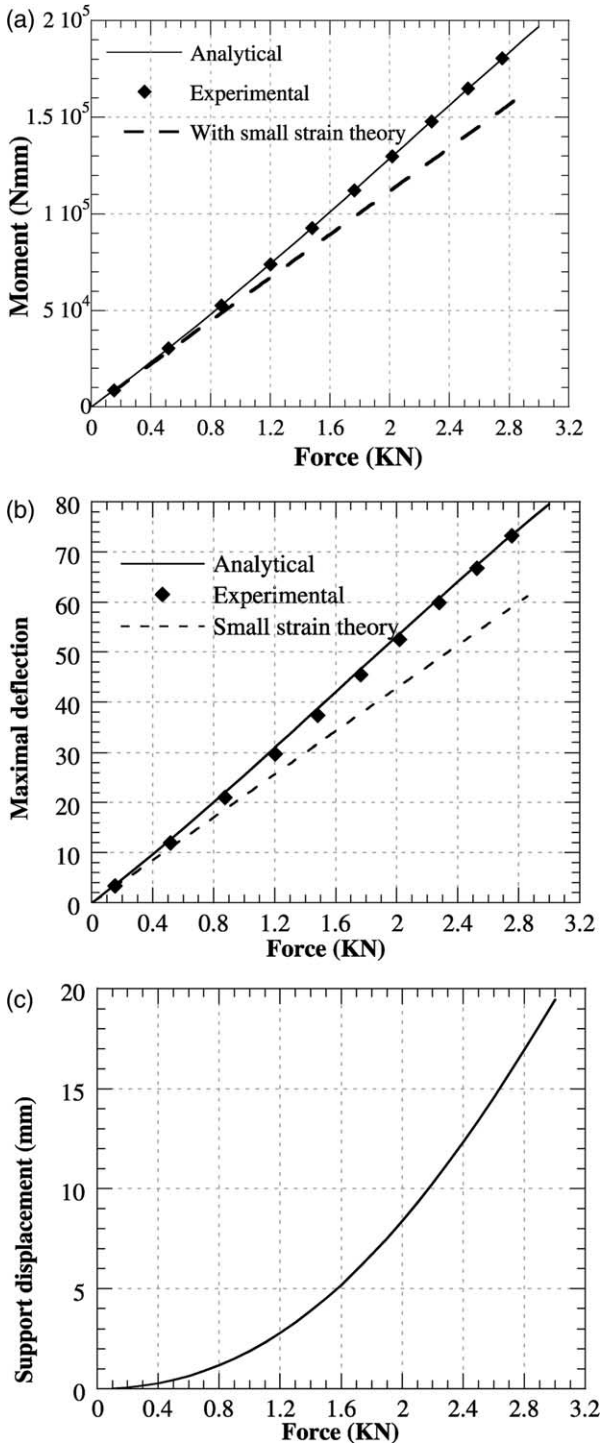

Fig. 11. (a) Bending moment versus loading force; (b) deflection versus loading force; (c) support displacement versus loading force.

- significant displacements and rotations on the level of the supports
- a symmetry of loading;
- a pure bending strain distribution;
- a real rigid body movement for the parts embedded by the sleeves.

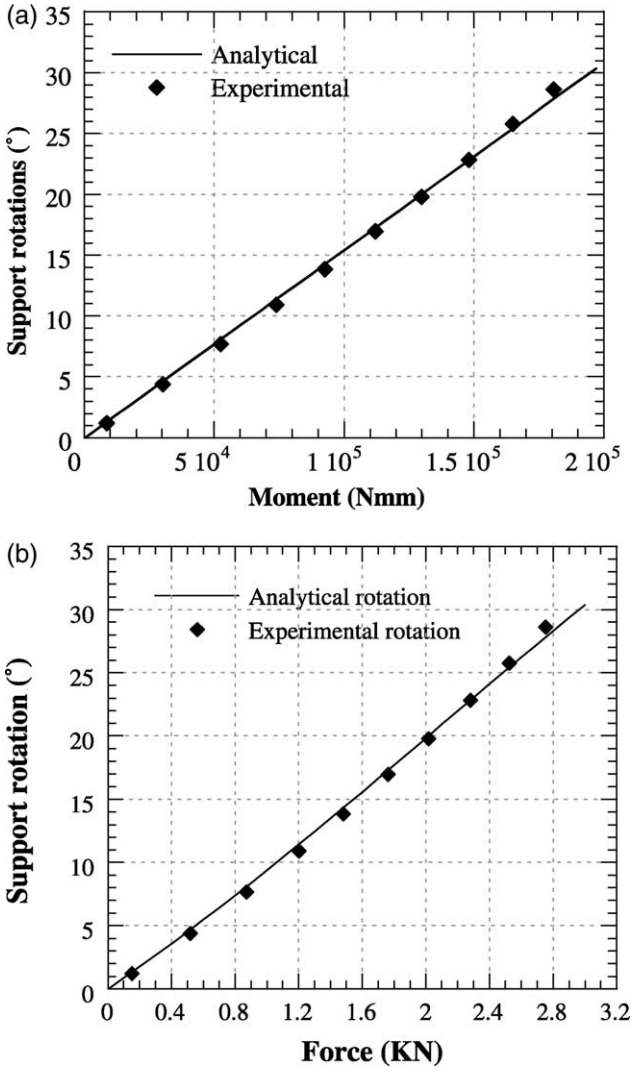

Fig. 12. (a) Support rotation versus bending moment; (b) support rotation versus loading force.

For analysis and validation we dissociated the global quantities, in order to check good test operation, of the local quantities, making a more accurate analysis possible of the real applied stress to the sample.

6.1. Global quantities

We presented the evolution of the applied bending moment, the maximum deflection and the support rotations, Figs. 11a–c and 12a,b, both for analytical and experimental results.

From these curves we observe

- A good correlation between the tests and the model.
- The non-linear state of the quantities, related to the finite transformations. This geometrical non-linearity is highlighted, for high loads, by the important differences between the results associated with the small deformation assumption, those with the analytical model and

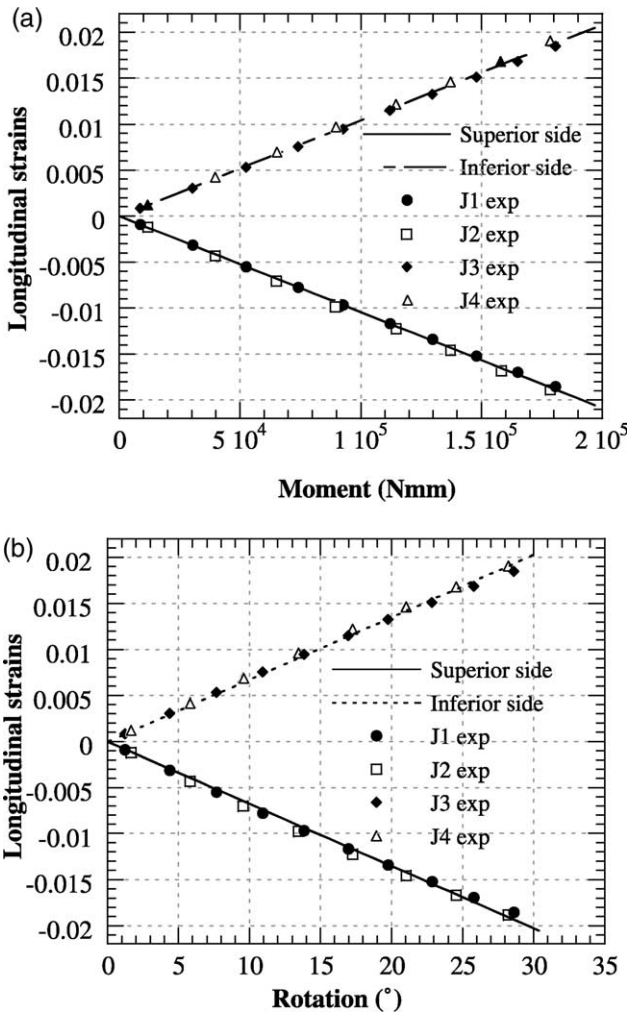

Fig. 13. (a) Longitudinal strains versus bending moment; (b) longitudinal strains versus support rotation.

the experimental results. For low loading, all the results are identical.

- Geometrical non-linearity is highlighted by the rather significant values of rotation and support displacements as well as by their evolutions according to the loading force.
- Rotation is linear versus the applied bending moment. This linearity is a significant property allowing a simple identification of elastic constitutive law coefficients. The appearances of non-linearities related to the behavior, damage, plasticity, etc can be rather easily highlighted with this device.

6.2. Local quantities

The evolution of the longitudinal strain versus the applied bending moment is linear. It is anti-symmetric compared to the median horizontal plane of the sample, Fig. 13a and b. Indeed the strains recorded in tension are quasi-identical to those in compression. Thanks to this device, it is possible to identify a difference in behavior related to damage only in the area loaded in tension. Moreover, the comparison of the strains recorded by various gauges shows that the stress is uniform along the length and the width of the sample. It is thus possible to detect material heterogeneities, which may appear and be propagated during loading. Such phenomena are very difficult to highlight in small deformations for flexible structures. The values obtained by the analytical model are very close to those measured experimentally, Fig. 13a and b.

In spite of the loaded sample flexibility, this new testing device applies a pure bending loading to the whole sample while avoiding unspecified premature damage elsewhere.

7. Fatigue bending tests on [− 5/85]s glass/epoxy samples

The geometrical characteristics of the samples are illustrated in Fig. 14. The manufacturing process of the composite plates allows us to have only layers stacked at 0 and 90° before cutting of samples. Consequently this process leads, after cutting the plates, to laminates of the type [0/90°], [− 5/85°], [− 10/80°] etc. In our case

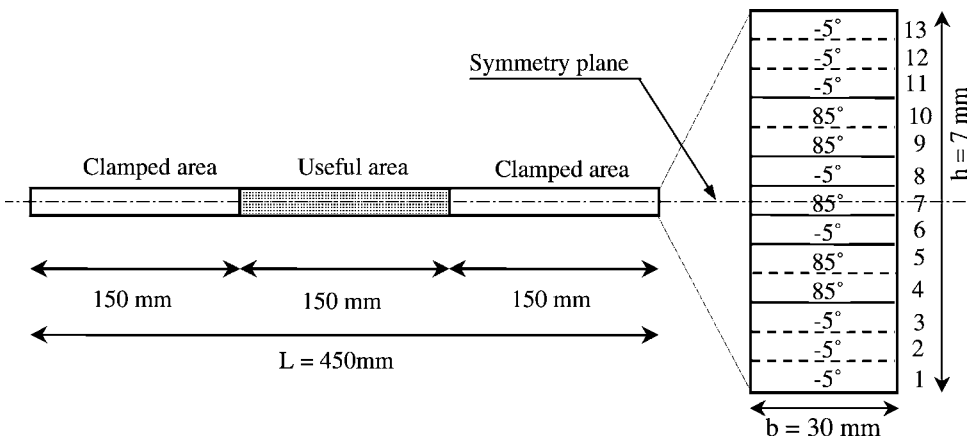

Fig. 14. Geometry of the samples and stacking sequences.

Table 2
Fatigue levels

Strain at failure = 1.8%	U (mm)
70% max = 1.2%	38
70% min = 0.4%	11
50% max = 0.9%	26
50% min = 0.3%	7
35% max = 0.6%	18
35% min = 0.2%	5

the laminate is symmetrical and is not balanced. It comprises an odd number of layers. It has 13 plies with 7 mm thickness. In order to obtain a complex stress in the elementary layers when the sample is pure bending loaded, an analysis of the effect of fiber orientation was carried out using the laminate theory. These investigations led to a stacking whose sequence is illustrated in Fig. 14, [6].

The experimental loading conditions are the following:

- Frequency: 2 Hz.
- Undulate loading ratio: $R = 0.3$.
- Control: displacement
- Maximal number of cycles: 1 million.

In order to establish the S–N curve, the definition of the fatigue loading is based on the static tests, the goal being to determine maximal and minimal imposed displacement levels in fatigue for a stress ratio ($\sigma_{min}/\sigma_{max}$) equal to 0.3. Consequently the average value of the ultimate strain is used. Levels with 70, 50, 35 and 30% were calculated compared to this rupture limit in static. The levels of imposed displacement are then deduced by using the non-linear curves representing the displacement of the jack

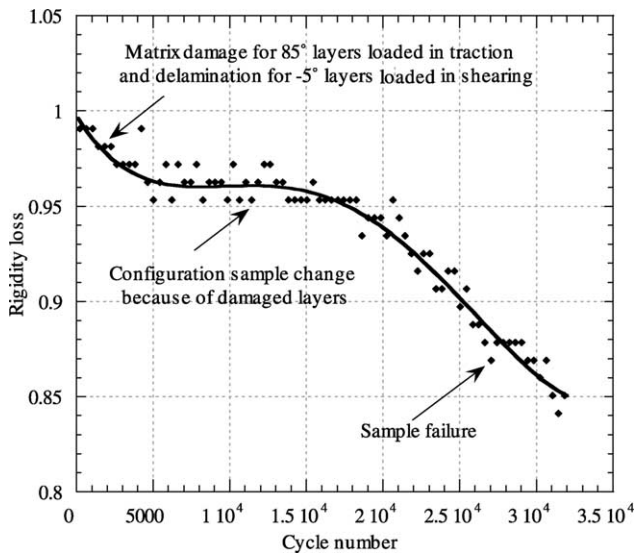

Fig. 15. Rigidity loss curve.

Table 3
Summary of the fatigue tests in pure bending

Sample	Level (%)	F_0 max (KN)	N delam	N 5%	N 10%
15-7	70	1.51	350	370	1540
15-4	70	1.48	820	610	1075
14-1	70	1.56	450	490	2485
15-1	50	1.07	21,000	17,800	25,200
14-6	50	1.11	44,960	22,500	52,500
15-10	50	1.16	72,000	18,700	57,000
8-7	35	0.84	No delami	320,000	1,200,000
13-4	35	0.80	No delami	580,000	990,000
13-1	35	0.84	370,000	350,000	1,245,000
12-10	30	0.70	No delami	Stopped at 10^6	Stopped at 10^6

versus the longitudinal strain in the sample. Imposed average displacements are given in Table 2.

Four loading levels were tested on samples resulting from varied plates in order to quantify the dispersion of the results in fatigue. The rigidity loss curves are strongly non-linear. They initially have a low slope followed by a violent rigidity loss corresponding to damage by shearing of the 5° layers. This is then followed by a plateau. Indeed, after the damage and especially the delamination of the 5° layers, the sample changes its configuration. This change is at the origin of the plateau of rigidity, Fig. 15. All the test results are gathered in Table 3. N_{delam} corresponds to the number of cycles when delamination appeared in the $-5°$ layers.

The pseudo Wöhler curve (expressed in displacement) is represented in Fig. 16. Little scatter is noticed in these tests. The tests related to the first level of loading correspond to the limit of the low cycle fatigue.

8. Conclusions and prospects

An original device allowing a pure bending load in large transformations has been presented in this paper, making it

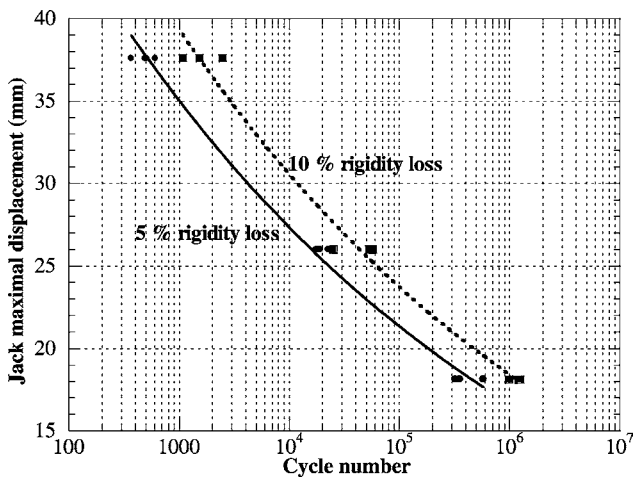

Fig. 16. Wöhler curve at 5 and 10% of rigidity loss.

possible to preserve stress homogeneity during loading even for rotations of about 35° at supports and a maximum deflection approximately equal to the useful sample length. Loading parameters are perfectly controllable and depend only on the instruction of the tensile testing machine and the geometry of the bench.

A beam model in large transformations is developed. It makes possible to optimize device dimensioning and its validation. The reference of the validation is experimental tests, using this device, on a series of glass–epoxy samples whose behavior was identified.

The device was then used to carry out fatigue tests on a series of glass–epoxy samples. These experimental tests were used to study the fatigue behavior of such a laminate and to identify some parameters associated with a numerical model, [6,7]. This latter predicts a structure lifetime made up of the same material and loaded under the same conditions as the sample.

The interest of this new device, in addition to the identification of the elastic coefficients realizable in small deformations, is to study behavior or structural non-linearities, thus avoiding deformations related to the parasitic phenomena even under extreme exploitation conditions where classical bending benches showed their limits. Among the possible applications and as an example, it is possible to highlight, by this device, the damage effect, a plasticity or a difference between tension and compression on the total or local behavior of a given material or structure.

Acknowledgements

We thank V. Bobet and P. Lory for the research direction of Renault for the scientific contribution and the provision of the samples used for the validation tests. We thank also C. Pastoré and the Mechanical Department of Engineering for the IUT of Ville d'avray for the assistance with the design and the realisation of the experimental device.

References

[1] Ben Zineb T. Analyse des zones à forts gradients de contraintes dans les plaques composites élancées à profil variable. PhD Thesis. ENSAM, Paris; January 1996.

[2] Chen ZQ, Agar TJ. Geometrical non-linear analysis of flexible spatial beam structures. Comput Struct 1993;49(N(6):1083–94.

[3] Simo JC, Hjelmstad KD, Taylor RL. Numerical formulations of elasto-viscoplastic response of beams accounting for the effect of shear. Comput Meth Appl Mech Engng 1984;42:301–30.

[4] Simo JC. A finite strain beam formulation. The three-dimensional dynamic problem. Part I. Comput Meth Appl Mech Engng 1985;49: 55–70.

[5] Simo JC. A three-dimensional finite-strain rod model. Part II. Computational aspects. Comput Meth Appl Mech Engng 1986;58:79–116.

[6] Sedrakian A. Contribution à la modélisation du comportement en fatigue des pièces composites stratifiés. PhD Thesis. ENSAM, Paris; May 2000.

[7] Sedrakian A, Ben Zineb T, Billoet JL. Contribution of industrial composite parts to fatigue behaviour simulation. International Journal of Fatigue 2002;24(3-4):307–18.

[8] Vittecoq E. Sur le comportement en compression des composites stratifiés Carbone–Epoxy. PhD Thesis. Paris VI; February 1991.